Biomedicine & Pharmacotherapy 97 (2018) 778–783

Contents lists available at ScienceDirect

Biomedicine & Pharmacotherapy

journal homepage: www.elsevier.com/locate/biopha

Original article

Targeting Akt as strategy to kill cancer cells using 3-substituted 5-anilinobenzo[*c*]isoxazolequinones: A preliminary study

Julio Benites[a,b,*], Jaime A. Valderrama[a,b], Maryan Ramos[a], Giulio G. Muccioli[c], Pedro Buc Calderon[a,d,*]

[a] *Facultad de Ciencias de la Salud, Universidad Arturo Prat, Casilla 121, Iquique, Chile*
[b] *Instituto de Ciencias Exactas y Naturales, Universidad Arturo Prat, Casilla 121, Iquique, Chile*
[c] *Bioanalysis and Pharmacology of Bioactive Lipids Laboratory, Louvain Drug Research Institute, Université catholique de Louvain, Brussels, Belgium*
[d] *Research Group in Metabolism and Nutrition, Louvain Drug Research Institute, Université catholique de Louvain, Belgium*

ARTICLE INFO

Keywords:
Hsp90
Akt
Cancer cells
Heterocyclic quinones
Benzo[*c*]isoxazolequinones
Amination reactions

ABSTRACT

Several new 3-substituted 5-anilinobenzo[*c*]isoxazolequinones were synthesized from 1,4-benzoquinone and alkyl- or arylcarbaldehydes by a three-step synthetic sequence. The new compounds (**3a-h**) were tested *in vitro* in normal human fibroblasts and two cancer cell lines for their cytotoxic activity. The range of IC_{50} values obtained for the compounds was from 3.4 to 74.2 μM. Five members of the series (**3b, 3d, 3e, 3f, 3g**) were further selected and evaluated as inhibitors of the Hsp90 chaperoning function taking Akt as example of Hsp90 client proteins. We also evaluated the changes of intracellular levels of GSH and ATP as markers of cellular metabolic status in response to these compounds in T24 cells. One of such isoxazolquinones (**3b**) decreased the expression of Akt, PARP and Hsp90. Compounds **3b** and **3d** decreased the amount of ATP but caused no effect on GSH levels. These compounds also activated caspase-3 but an apoptosis-like type of cell death was unlike since PARP protein was not cleaved and caspase activation was substantially lower than its activation induced by staurosporine, a known caspase-3 activator in T24 cells.

Taken together, preliminary results led to the discovery of an original lead compound (**3b**) which can be used as model to obtain new Akt inhibitors.

1. Introduction

Heat shock proteins (HSPs) ensure protein homeostasis in the presence and in the absence of cellular stress. In the event of protein damage, these molecular chaperones facilitate protein refolding or target the protein for degradation if the damage to the protein is irreversible [1]. Among chaperones, Hsp90 is unique because most of its client proteins are conformationally labile signal transducers that play a crucial role in cell growth control, survival and development processes [2]. Hsp90 represents 1–2% of the total protein cellular content but its expression is enhanced by 2–10-fold in cancer cells [3], thus making it an attractive target for the development of therapeutic inhibitors [1,4–6].

Several reasons make Hsp90 a very promising and relevant target in cancer therapy. For instance, Hsp90 is required for the stability and/or activity of many client proteins that play essential roles in cancer cells such as Bcr-Abl, BRAF, Akt, mutated p53, telomerase, *etc.* [1]. In addition, cancer cells are addicted to oncoproteins [7]. These latter proteins are often expressed as mutant forms which are more dependent on Hsp90 for their stability than their normal counterparts. Finally, Hsp90 inhibitors bind preferentially to Hsp90 in cancer cells rather than in normal cells [8].

Most of Hsp90 inhibitors tested in clinics share a common mechanism of action that involves their competitive binding to the N-terminal nucleotide binding site of Hsp90 [9]. In this context, we developed an original strategy targeting the chaperone function of Hsp90 by inducing oxidative cell stress. Indeed, the association of ascorbate and menadione (Asc/Men), a H_2O_2-generating system [10–12], inhibits Hsp90 activity by promoting oxidative protein cleavage, which causes degradation of its client proteins [13]. In addition, we proposed that such Hsp90 cleavage followed by Bcr-Abl degradation, is a very efficient approach to overcome cell resistance to imatinib in K562 cells expressing the T315I mutated form of Bcr-Abl [4,13–15].

We designed molecules containing the 1,4 naphthoquinone scaffold

Abbreviations: Hsp90, heat shock protein of 90 kDa; Asc/Men, ascorbate/menadione; ROS, reactive oxygen species; NMR, nuclear magnetic resonance spectroscopy; HRMS, High Resolution Mass Spectrometry; DMSO, dimethylsulfoxide; PBS, phosphate buffer saline; MTT, 3-(4,5-dimethylthiazol-2-yl)-2,5-diphenyltetrazolium bromide

* Corresponding authors at: Facultad de Ciencias de la Salud, Universidad Arturo Prat, Casilla 121, Iquique, Chile.
E-mail addresses: juliob@unap.cl (J. Benites), pedro.buccalderon@uclovain.be (P. Buc Calderon).

http://dx.doi.org/10.1016/j.biopha.2017.10.108
Received 22 August 2017; Received in revised form 19 October 2017; Accepted 21 October 2017

as potential Hsp90 inhibitors. The rationale of this choice is based on the reported ability of 2,3-substituted 1,4 naphthoquinones to inhibit Hsp90 [16] and also on our previous data obtained with the association of ascorbate and menadione (2-methyl-1,4 naphthoquinone). We found that 3-acyl-2-arylamino-1,4-naphthoquinones (in the presence of ascorbate), are also able to induce Hsp90 protein cleavage and a necrosis-like cell death in K562 cells [17]. Moreover, it was concluded that oxidative Hsp90 cleavage was provoked by an *in situ* reactive oxygen species (ROS) formation and not due to proteolysis just preceding cell death [17].

As a continuation of our research efforts in finding new cytotoxic quinoid agents, we were interested in a series based on the 5-anilinobenzo[*c*]isoxazolequinone scaffold. The new target series was designed on the basis of the structure of cytotoxic 2-anilinonaphthoquinones [18,19], *N*-heterocyclic analogues [20] and fused isoxazol-containing naphthoquinones which induce *in vitro* cytotoxicity in cancer cells and also act as inhibitors of Hsp90 [21]. Herein we report preliminary results on the synthesis of a number of 5-anilinobenzo[*c*]isoxazolequinone and the assessment of their potential cytotoxicity on cancer cell lines. Moreover, also reported are the effects of 5-anilinobenzo[*c*]isoxazolequinones on the inhibition of Hsp90 chaperoning function, on caspase-3 activity and on PARP protein integrity as apoptosis markers. We also report some metabolic indexes such as intracellular contents of ATP and reduced glutathione (GSH) evaluation.

2. Materials and methods

2.1. Synthesis of 3-alkyl- and 3-aryl-5-anilinobenzo[c]isoxazol-4,7-quinones

The preparation of the selected precursors **1a-h** (Fig. 1) was carried out by solar-chemical photo-Friedel–Crafts acylation of 1,4-benzoquinone with the following aldehydes: ethanal; butanal; hexanal; octanal; 3,4-dimethoxybenzaldehyde; 3,4,5-trimethoxybenzaldehyde; furan-2-carbaldehyde and thiophene-2-carbaldehyde according to a previously published procedure [22]. The preparation of the 3-acyl-2,5-dianilino-1,4-benzoquinones **2a-h** was accomplished by oxidative amination of 2-acylbenzoquinones with aniline by modification of a procedure described in literature [23]. Further reaction of benzoquinones **2a-h** with hydroxylamine in ethanol furnished the corresponding 5-anilinobenzo [*c*]isoxazol-4,7-quinones **3a-h**. The structures of all new compounds were determined by IR, ^{1}H-, ^{13}C NMR and HRMS. Data of compounds **3a-h** are listed in the enclosed Supplementary files.

All the solvents and reagents were purchased from Aldrich (St. Louis, MO, USA) and Merck (Darmstadt, Germany) and were used as supplied. Melting points were determined on a Stuart Scientific SMP3 (Staffordshire, UK) apparatus and values reported are uncorrected. The IR spectra were recorded on an FT IR Bruker spectrophotometer, model Vector 22 (Bruker, Rheinstetten, Germany), using KBr disks. ^{1}H NMR spectra were recorded on a Bruker Avance-400 instrument (Bruker) in deuterated dimethyl sulfoxide (DMSO-d_6) and deuterochloroform ($CDCl_3$). ^{13}C NMR spectra were obtained in DMSO-d_6 and $CDCl_3$ at 100 MHz. Bidimensional NMR techniques and distortionless enhancement by polarisation transfer (DEPT) were used for signal assignment. Chemical shifts are expressed in ppm downfield relative to tetramethylsilane and the coupling constants (*J*) are reported in Hertz. The HRMS data were obtained using a LTQ-Orbitrap mass spectrometer (Thermo-Fisher Scientific, Waltham, MA 02454, USA) with the analysis performed using an atmospheric-pressure chemical ionization (APCI) source operated in positive mode. Silica gel Merck 60 (70–230 mesh, from Merck) was used for preparative column chromatography and TLC aluminum foil $60F_{254}$ for analytical thin layer chromatography (TLC).

2.2. Cell lines and cell culture

Human cancer cell lines T24 (bladder), DU-145 (prostate) and non-tumor fibroblasts AG 1523 were obtained from the American Type Culture Collection (ATCC, Manassas, VA, USA). The cultures were maintained at a density of 1–2 × 10^5 cells/mL and the medium was changed at 48- to 72-h intervals. They were cultured in high-glucose Dulbecco's modified Eagle medium (Gibco, Grand Island, NY, USA) supplemented with 10% fetal calf serum, penicillin (100 U/mL), and streptomycin (100 µg/mL). All cultures were kept at 37 °C in 95% air/5% CO_2 at 100% humidity. Phosphate-buffered saline (PBS) was purchased from Gibco. Cells were incubated at the indicated times at 37 °C with or without quinones at various concentrations.

2.3. Cell survival assays

The cytotoxicity of the quinones was assessed by following the reduction of MTT (3-(4,5-Dimethylthiazol-2-yl)-2,5-diphenyltetrazolium bromide) to formazan blue [24]. Cells were seeded into 96-well plates at a density of 10 000 cells/well for 24 h and then incubated for 48 h with or without the quinone derivatives. Doxorubicin was used as standard chemotherapeutic agent (positive control). Cells were then washed twice with warm PBS and incubated with MTT (0.5 mg/mL) for 2 h at 37 °C. Blue formazan crystals were solubilized by adding 100 µl DMSO/well, and the optical density of coloured solutions was

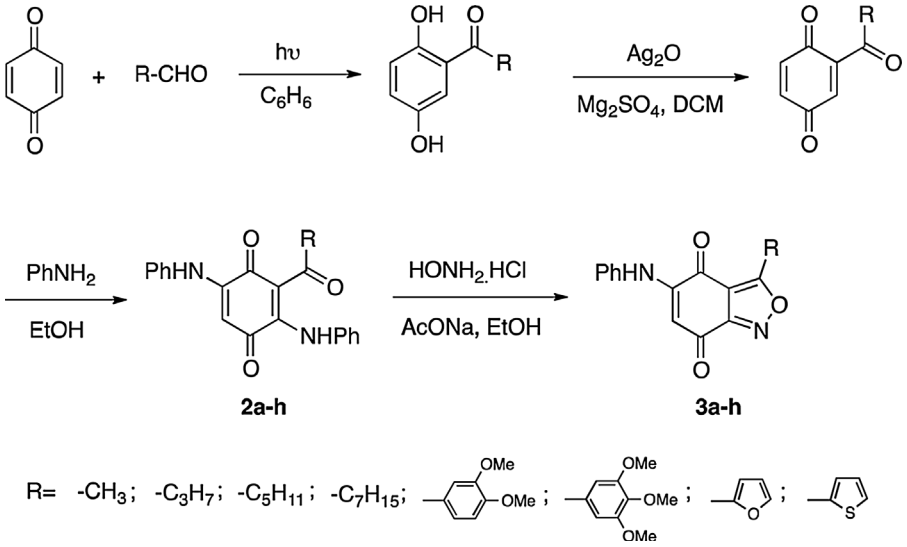

Fig. 1. Scheme of synthesis pathway of 3-alkyl- and 3-aryl-5-anilinobenzo[*c*]isoxazol-4,7-quinones.
Friedel-Crafts photo acylation of 1,4-benzoquinone with aldehydes leads to acylhydroquinones **1a-h**. They were further oxidized with silver oxide and the further reaction with aniline yield the substituted benzoquinones **2a-h**. The final reaction with hydroxylamine leads to compounds **3a-h**.

Table 1
IC_{50} values (μM) of **3a-h** on T24 (bladder) and DU-145 (prostate) and AG1523 fibroblasts.

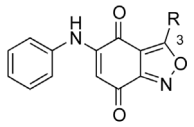

3a-h

Quinone	R	T24	DU-145	Mean value	AG 1523
3a	$-CH_3$	> 100	> 100	NC	> 100
3b	$-C_3H_7$	53.5 ± 2.7	9.8 ± 0.66	31.6	> 100
3c	$-C_5H_{11}$	> 100	> 100	NC	> 100
3d	$-C_7H_{15}$	13.1 ± 0.8	28.4 ± 2.5	20.7	> 100
3e	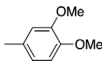	10.4 ± 1.1	15.3 ± 1.3	12.8	> 100
3f	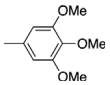	15.1 ± 1.2	27.5 ± 2.1	21.3	40.7 ± 3.4
3g		3.4 ± 0.3	74.2 ± 3.6	38.8	29.6 ± 1.9
3h		15.4 ± 1.4	> 100	NC	30.1 ± 2.5
DOXO	–	0.46 ± 0.08	0.93 ± 0.06	0.69	0.53 ± 0.05

Cells were seeded into 96-well plates at a density of 10 000 cells/well for 24 h and then incubated for 48 h with or without the quinone derivatives. At the end of the incubation, aliquots of cells suspension were taken and the MTT test was performed as described in the Materials and Methods section. Results are expressed as means values ± SEM (n = 3). DOXO = doxorubicin.

subsequently read at 550 nm. Results are expressed as% of MTT reduction compared to untreated control conditions. The IC_{50} values were calculated using the GraphPad Prism software (San Diego, CA, USA).

The caspase-3 activity was monitored by cleavage of a specific peptide substrate, Asp-Glu-Val-Asp-AFC (DEVD-AFC) as reported elsewhere [11,12]. Staurosporine (1 μM) was used as positive control [25]. Briefly, after 6 h of incubation with quinones, T24 cells were washed twice with PBS, lysed and homogenates were centrifuged at 14,000 × *g* for 10 min at 4 °C. The supernatants were incubated with DEVD-AFC substrate; luminescence due to fluorochrome release was recorded at room temperature in a LS50B luminescence spectrometer (375 nm excitation, 510 nm emission). Results are expressed as Units/mg protein, corresponding to the cleavage of 1 pmol of DEVD-AFC per min at 25 °C and at saturation substrate concentrations. Protein amounts were calculated using the method of Bradford.

2.4. Immunoblotting procedures

At the indicated times, T24 cells were washed twice with ice-cold PBS and then resuspended in RIPA lysis buffer supplemented with 1% Protease Inhibitor Cocktail (Sigma–Aldrich) and 3% Phosphatase Inhibitor Cocktail (Calbiochem). The samples were kept on ice for 20 min, centrifuged at 13,000 × *g* for 20 min at 4 °C and then stored at −20 °C. Equal amounts of proteins (20–30 μg) were subjected to SDS-PAGE (6–15% separating gel) followed by electroblot to nitrocellulose membranes. The membranes were blocked for 1 h in TBS buffer (pH 7.4) containing 5% powdered milk protein and then incubated overnight at 4 °C with the appropriate antibody. Rabbit polyclonal antibodies against PARP were from Santa Cruz Biotechnology (Santa Cruz, CA, USA). Mouse monoclonal antibodies against Hsp90α/β C-terminus, Akt (05-591) and β-actin were purchased from Santa Cruz Biotechnology (Santa Cruz, CA, USA); Millipore (Merck KGaA, Darmstadt, Germany) and Abcam (Cambridge, UK), respectively. After washing steps, membranes were exposed for 60 min at room temperature to secondary antibodies either from mouse (Dako, Glostrup, Denmark) or rabbit (Chemicon International, Temecula, CA) coupled to horseradish peroxidase. Finally, the protein bands were detected by chemiluminescence using the Pierce ECL detection (Rockford, IL, USA).

Table 2
Yields, half-wave potentials ($E^I_{½}$), lipophilicity (ClogP) and molar refractivity (CMR) values of quinones **3a**-**3h**.

Quinone	Clog P	- $E^I_{½}$ (mV)	CMR (cm^3/mol)
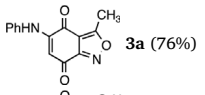 **3a** (76%)	0.48	680	72.55
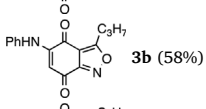 **3b** (58%)	1.39	890	81.75
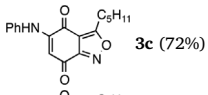 **3c** (72%)	2.22	1090	90.95
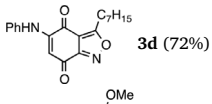 **3d** (72%)	3.06	1100	100.15
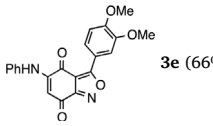 **3e** (66%)	1.63	760	106.75
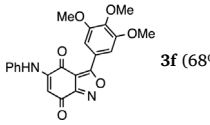 **3f** (68%)	1.50	780	114.00
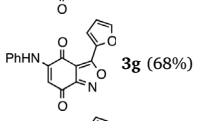 **3g** (68%)	0.49	1280	84.77
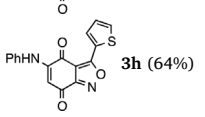 **3h** (64%)	1.86	1360	90.24

The lipophilicity (Clog P) and Molar Refractivity (CMR) were estimated using the CSChem 3D software. The half-wave potentials ($E^I_{½}$) were measured by cyclic voltammetry in acetonitrile as a solvent at room temperature, using a platinum electrode and 0.1 M tetraethylamoniumtetrafluoroborate as the supporting electrolyte. The voltammograms were run in the potential range 0.0–2.0 V *versus* non-aqueous Ag/Ag+.

2.5. Intracellular levels of GSH and ATP

Intracellular GSH was estimated according to Griffith [26]. Briefly, T24-treated cells were washed with cold PBS and immediately acidified with 5% sulfosalicylic acid. The samples were submitted to two freeze-thaw cycles and centrifuged at 4 °C (10.000 × *g* for 10 min). Furthermore, 10 μl of the supernatant were placed in a mixture at pH 7 containing 0.2 U/ml of glutathione reductase, 50 mg/mL of dithionitrobenzoic acid (DTNB) and 1 mM EDTA. The reaction was initiated by adding NADPH (50 mM) and changes in absorbance were recorded at 412 nm. Results are expressed as nmol/mg of protein. Protein amounts were calculated using the method of Bradford.

ATP content was calculated by using the Roche ATP Bioluminescence Assay kit CLS II (Mannheim, Germany) following the procedures given by the suppliers. Results are expressed as nmol/10^6 cells.

2.6. Data analysis

All experiments were performed at least 3 times and groups were compared by ANOVA test using GraphPad Prism software (San Diego, CA, USA). ANOVA test was followed by Bonferroni's multiple comparison test. The level of significance was set at $p < 0.05$.

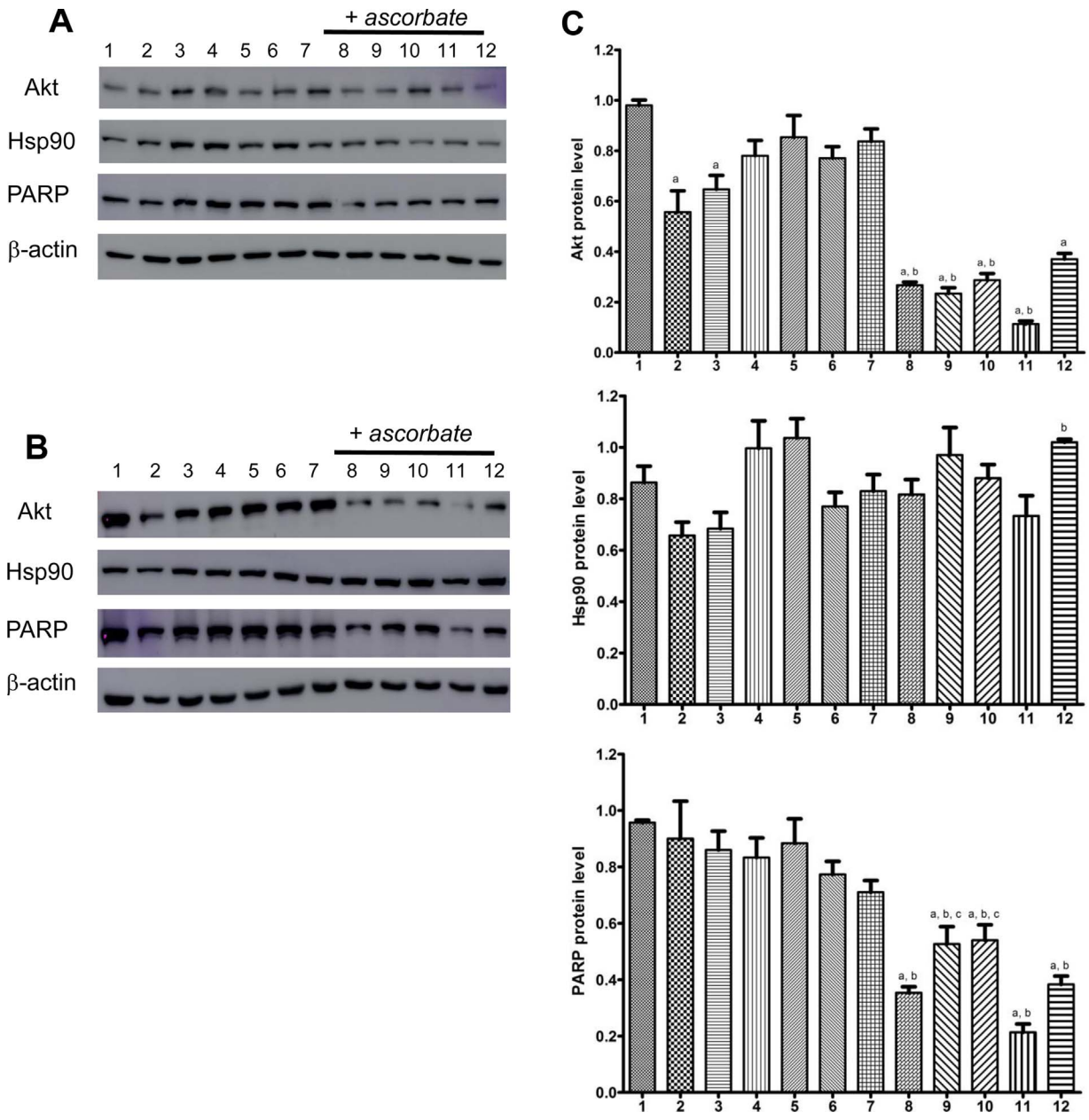

Fig. 2. The effect of quinones on Akt, Hsp90 and PARP protein expression in human prostate-derived T24 cancer cells.
T24 cells were incubated for 4 (3 A) and 24 h (3 B) in the absence (lanes 1–7) or presence of 1 mM vitamin C (lanes 8–12), and different quinones at the concentration of 5 μM. Quinones were added either alone **3f** (3), **3e** (4), **3g** (5), **3b** (6), **3d** (7) or together with 1 mM of vitamin C: **3f** (8), **3e** (9), **3g** (10), **3b** (11), **3d** (12). β-actin was used as loading control. Densitometry for each protein band was carried out only for experiments at 24 h, and they are represented in Fig. 2C.
(a) $p < 0.05$ as compared to control values
(b) $p < 0.05$ as compared to obtained in cells cells treated with ascorbate
(c) $p < 0.05$ as compared to values obtained in cells treated with **3b** + ascorbate

3. Results

The cytotoxic activity of quinones **3a-h** was evaluated in two human cancer cell lines, namely T24 (bladder) and DU-145 (prostate), and in a healthy non-tumor cell line, the human-derived fibroblasts AG1523 (Table 1). The comparison of the IC_{50} values reported in Table 2, indicates that both cancer and non-tumor cells show a huge range of sensitivities against different quinones. For instance, excepting values > 100 μM, IC_{50} values from 3.4 to 53.5 μM were obtained in T24 cells, and in the case of DU-145 cell line, the obtained IC_{50} values ranged between 9.8 and 74.2 μM. It is noteworthy that doxorubicin was more active than quinones but its cytotoxicity was observed not only in tumor cells but also in non-tumor human fibroblasts.

Since the main structural difference of the designed 5-anilinobenzo [*c*]isoxazol-4,7-quinones **3a-h** is the aliphatic or aromatic nature of the substituent located at C-3, we evaluated the influence of this factor on the cytotoxic activity. As shown in Table 1, the mean cytotoxic potency follows the order: **3e** > **3d** > **3f** > **3b** > **3g** (R = 3,4-dimethoxyphenyl > heptyl; 3,4,5-trimethoxyphenyl > propyl > furyl). The cytotoxic potency observed for the different compounds clearly indicates that the lipophilicity (ClogP) and the first half-wave potentials ($E^{I}_{½}$), as reported in Table 2, do not influence the magnitude of the observed cytotoxic effects. Interestingly, the closer magnitude of the molar refractivity descriptor (CMR) of the two most active members of the series (**3d** and **3e**) suggests that the volume and polarizability of these molecules may contribute to the biological action mechanism

Table 3
Effect of quinones on caspase-3 activity and intracellular levels of ATP and GSH.

Compounds	ATP (nmol/10^6 cells)	GSH (nmol/mg protein)	DEVDase activity (U/mg protein)
none	5.1 ± 0.61	7.14 ± 1.02	14.2 ± 1.75
3b	3.1 ± 0.38*	6.88 ± 1.83	21.5 ± 2.85*
3d	3.5 ± 0.34*	8.73 ± 1.69	18.9 ± 1.44*
3e	6.2 ± 0.61	6.10 ± 1.38	11.7 ± 1.75
3f	4.1 ± 0.35	8.74 ± 1.35	14.3 ± 2.34
3g	4.3 ± 0.34	6.45 ± 1.53	17.5 ± 1.07
Staurosporine	n.t.	n.t.	308.8 ± 16*

T24 cells were incubated for 6 h in the absence or in the presence of quinones (5 μM) and staurosporine (1 μM). Aliquots of cell suspensions were taken and samples processed as reported in the Materials and Methods section.

* $p < 0.05$ as compared to control untreated cells.

mediated by compounds **3d** and **3e**, respectively. In terms of structure-activity relationship, 5-anilino-3-(3,4-dimethoxyphenyl)benzo[*c*]isoxazol-4,7-quinone (**3e**) showed the most potent cytotoxic activity *in vitro* compared to the other congeners of the series, indicating a correlation that may offer an insight into the mode of action of these compounds.

Compounds **3b**, **3d, 3e, 3f** and **3g** were selected for further assays performed only in T24 cells because such cell line was about two-fold more sensitive to quinones compared to DU-145 cells. Therefore, the potential inhibitory effects of the selected chemotypes on the chaperone activity of Hsp90 protein (including the effects on the stability of its client proteins) were investigated in T24 cells and further assessed by Western blot.

Fig. 2A shows no significant changes in the expression of Akt, Hsp90 and PARP proteins in cells incubated for 4 h either with quinones alone or together with 1 mM sodium ascorbate (Vitamin C). However, when cells were incubated for 24 h with quinones plus vitamin C, dramatic changes in the expression of some proteins were observed (Fig. 2B). Akt and PARP proteins were sensitive to all quinones in the presence of ascorbate with diverse efficacy. For instance, in the presence of ascorbate, compound **3b** was the most active (lane 11, Fig. 2B) reducing the AKT and PARP protein levels by more than 80% as compared to control conditions (Fig. 2C). Interestingly, Hsp90 protein was not modified by any of the quinones either alone or in the presence of ascorbate and no oxidative cleavage was produced as in the case of Asc/Men [13,14].

Table 3 shows that cytotoxicity caused by quinones on cancer cells was not due to a caspase-dependent cell death since the activity of caspase-3 was not modified by any of the quinones used in this assay. Indeed, although quinones **3b** and **3d** enhanced by 1.5- and 1.3-fold the enzyme activity, respectively, such increase should not be considered as a biologically-relevant activation of caspase because staurosporine, a positive inducer of apoptosis in T24 cells [25], provoked more than 20-fold increase of enzyme activity. In addition, both quinones (**3b** and **3d**) caused a 30–40% decrease in ATP. Together, it is unlikely that quinones **3b** and **3d** could trigger apoptosis, as this is an ATP-dependent process (Table 3). Additionally, neither PARP cleavage (Fig. 2) nor intracellular levels of GSH were changed upon different quinone treatments.

4. Discussion

The therapeutic use of Hsp90 inhibitors such as geldanamycin and others, is based on the blockage of ATP binding to the N-terminal domain, an inhibitory process that is accompanied by proteolysis of several Hsp90 client proteins [13,15,27].

We have recently developed an original approach to cleave Hsp90 by using a pro-oxidant treatment that generates H_2O_2, which induces oxidative stress, namely the association of ascorbate and menadione (Asc/Men). Such oxidative protein cleavage is followed by Hsp90-dependent oncoproteins degradation [13] and likely to be produced within the N-terminal nucleotide binding site by an oxidative-mediated process [13,14]. The decreased levels of Akt are not due to a loss of chaperoning function of Hsp90 since Akt drop is occurring without Hsp90 degradation. It is noteworthy that Akt is an Hsp90 client protein that plays a critical role in the PI3Kinase pathway. Since such signaling pathway is unregulated in most of cancers [28], several efforts have been made to design specific Akt inhibitors. Since the anti-apoptosis effect is mediated by the PI3Kinase signaling pathway, the results obtained in this study are in line with such attempts and the construction of a robust series of 3-aryl-5-anilinobenzoisoxazolequinones as putative Akt inhibitors is currently under way.

On the other hand, the decreased expression of PARP in T24 cells is not associated with the induction of apoptosis since no caspase activation was observed in these cells (Table 3). In addition, since PARP protein, a well-known caspase-3 substrate [29] was not cleaved and ATP levels – required to trigger the apoptosis process [30] – were decreased, the induction of an apoptotic process is rather unlikely.

5. Conclusion

Akt and its signaling pathway could be targeted to kill cancer cells. The heterocyclic quinone scaffold may be modulated to yield new and potent Akt inhibitors as shown by **3b**. In addition, compounds **3d** and **3e**, containing alkyl and aryl substituents at the 3-position of the scaffold, displayed an interesting anticancer activity.

Acknowledgements

We express our gratitude to Veronique Allaeys for her excellent technical assistance and to Fondo Nacional de Ciencia y Tecnología (Grant No. 1150030 to JB) for the financial support given to this study.

Appendix A. Supplementary data

Supplementary data associated with this article can be found, in the online version, at https://doi.org/10.1016/j.biopha.2017.10.108.

References

[1] F.H. Schopf, M.M. Biebl, J. Buchner, The Hsp90 chaperone machinery, Nat. Rev. Mol. Cell Biol. 18 (2017) 345–360.
[2] W.B. Pratt, The Hsp90-based chaperone system: involvement in signal transduction from a variety of hormone and growth factor receptors, Proc. Soc. Exp. Biol. Med. 217 (1998) 420–434.
[3] L. Neckers, Hsp90 inhibitors as novel cancer chemotherapeutic agents, Trends Mol. Med. 8 (2002) S55–S66.
[4] R. Beck, N. Dejeans, C. Glorieux, R. Curi Pedrosa, D. Vasquez, J.A. Valderrama, P. Buc Calderon, J. Verrax, Molecular chaperone Hsp90 as a target for oxidant-based anticancer therapies, Curr. Med. Chem. 18 (2011) 2816–2825.
[5] Z. Solárová, M. Kello, L. Varinská, M. Budovská, P. Solár, Inhibition of heat shock protein (Hsp) 90 potentiates the antiproliferative and pro-apoptotic effects of 2-(4′fluoro-phenylamino)-4H-1,3-thiazine[6,5-b]indole in A2780cis cells, Biomed. Pharmacother. 85 (2017) 463–471.
[6] L. Whitesell, E.G. Mimnaugh, C.B. De, C.E. Myers, L.M. Neckers, Inhibition of heat shock protein Hsp90-pp60v-src heteroprotein complex formation by benzoquinone ansamycins: essential role for stress proteins in oncogenic transformation, Proc. Natl. Acad. Sci. U. S. A. 91 (1994) 8324–8328.
[7] I.B. Weinstein, A. Joe, Oncogene addiction, Cancer Res. 68 (2008) 3077–3080.
[8] G. Chiosis, H. Hueso, N. Rosen, E. Mimnaugh, L. Whitesell, L. Neckers, 17-AAG: low target binding affinity and potent cell activity—finding an explanation, Mol. Cancer Ther. 2 (2003) 123–129.
[9] T. Taldone, A. Gozman, R. Maharaj, G. Chiosis, Targeting Hsp90: small-molecule inhibitors and their clinical development, Curr. Opin. Pharmacol. 8 (2008) 370–374.
[10] J. Verrax, J. Cadrobbi, C. Marques, H.S. Taper, Y. Habraken, J. Piette, P. Buc Calderon, Ascorbate potentiates the cytotoxity of menadione leading to an oxidative stress that kills cancer cells by a non-apoptotic caspase-3 independent form of cell death, Apoptosis 9 (2004) 223–233.
[11] J. Verrax, M. Delvaux, N. Beghein, H.S. Taper, B. Gallez, P. Buc Calderon, Enhancement of quinone redox cycling by ascorbate leads to cancer cell death through a caspase-3 independent pathway. An in vitro comparative study, Free Radic. Res. 39 (2005) 649–657.
[12] J. Verrax, J. Stockis, A. Tison, H. Taper, P. Buc Calderon, Oxidative stress by ascorbate/menadione association kills K562 human chronic myelogenous leukemia

cells and inhibits its tumor growth in nude mice, Biochem. Pharmacol. 72 (2006) 671–680.
[13] R. Beck, N. Dejeans, C. Glorieux, M. Creton, E. Delaive, M. Dieu, M. Raes, Ph. Leveque, B. Gallez, M. Depuydt, J.-F. Collet, P. Buc Calderon, J. Verrax, Hsp90 is cleaved by reactive oxygen species at a highly conserved N-terminal amino acid motif, PLoS One 7 (2012) e40795.
[14] R. Beck, J. Verrax, T. Gonze, M. Zappone, R. Curi Pedrosa, H. Taper, O. Feron, P. Buc Calderon, Hsp90 cleavage by an oxidative stress leads to its client proteins degradation and cancer cell death, Biochem. Pharmacol. 77 (2009) 375–383.
[15] R. Beck, R. Curi Pedrosa, N. Dejeans, C. Glorieux, Ph. Levêque, B. Gallez, H. Taper, S. Eeckhoudt, L. Knoops, P. Buc Calderon, J. Verrax, Ascorbate/menadione-induced oxidative stress kills cancer cells that express normal or mutated forms of the oncogenic protein Bcr-Abl An in vitro and in vivo mechanistic study, Invest. New Drugs 29 (2011) 891–900.
[16] M.K. Hadden, S.A. Davenport, R.L. Matts, B.S. Blagg, Synthesis and evaluation of Hsp90 inhibitors that contain the 1,4-naphthoquinone scaffold, Bioorg. Med. Chem. 17 (2009) 634–640.
[17] D. Rios, J. Benites, J. Valderrama, M. Farias, R.C. Pedrosa, J. Verrax, P. Buc Calderon, Biological evaluation of 3-acyl-2-arylamino-1,4-naphthoquinones as inhibitors of Hsp90 chaperoning function, Curr. Top. Med. Chem. 12 (2012) 2094–2102.
[18] J.A. Valderrama, A. Ibacache, J.A. Rodriguez, C. Theoduloz, J. Benites, Studies on quinones. Part 47. Synthesis of novel phenylaminophenanthridinequinones as potential antitumor agents, Eur. J. Med. Chem. 46 (2011) 3398–3409.
[19] J.A. Ibacache, V. Delgado, J. Benites, C. Theoduloz, V. Arancibia, G.C. Muccioli, J.A. Valderrama, Synthesis, half-wave potentials and antiproliferative activity of 1-aryl-substituted aminoisoquinolinequinones, Molecules 19 (2014) 726–739.
[20] F.A. Monsalve, J.A. Valderrama, D. Vásquez, A. Ibacache, J.A. Rodríguez, D.R. González, E. González, Inhibition of human topoisomerase I and activation of caspase-3 by aza-angucyclinones and arylaminopyrimido[4,5-c]isoquinoline-7,10-quinones, Int. J. Mol. Med. 30 (2012) 151–156.
[21] A. Bargiotti, L. Musso, S. Dallavalle, L. Merlini, G. Gallo, A. Ciacci, G. Giannini, W. Cabri, S. Penco, L. Vesci, M. Castorina, F.M. Milazzo, M.L. Cervoni, M. Barbarino, C. Pisano, C. Giommarelli, V. Zuco, M. De Cesare, F. Zunino, Isoxazolo(aza)naphthoquinones: a new class of cytotoxic Hsp90 inhibitors, Eur. J. Med. Chem. 53 (2012) 64–75.
[22] J. Benites, D. Ríos, P. Díaz, J. Valderrama, The solar-chemical photo-friedel-crafts heteroacylation of 1, 4-quinones, Tetrahedron Lett. 52 (2011) 609–611.
[23] M.J. Suto, M.A. Stier, R.Th. Winters, W.R. Turner, Ch.D. Pinter, W.E. Elliott, J.S. Sebolt-Leopold, Synthesis and evaluation of a series of 3,5-disubstituted benzisoxazole-4,7-diones, J. Med. Chem. 34 (1991) 3290–3294.
[24] T. Mosmann, Rapid colorimetric assay for cellular growth and survival: application to proliferation and cytotoxicity assays, J. Immunol. Methods 65 (1983) 55–63.
[25] M.V. Clement, S. Sivarajah, S. Pervaiz, Production of intracellular superoxide mediates dithiothreitol-dependent inhibition of apoptotic cell death, Antioxid. Redox Signal. 7 (2005) 456–464.
[26] O.W. Griffith, Determination of glutathione and glutathione disulfide using glutathione reductase and 2-vinylpyridine, Anal. Biochem. 106 (1980) 207–212.
[27] G. Garg, A. Khandelwal, B.S. Blagg, Anticancer inhibitors of Hsp90 function: beyond the usual suspects, Adv. Cancer Res. 129 (2016) 51–88.
[28] B. Vanhaesebroeck, J. Guillermet-Guibert, M. Graupera, B. Bilanges, The emerging mechanisms of isoform-specific PI3K signaling, Nat. Rev. Mol. Cell Biol. 11 (2010) 329–341.
[29] J.C. Timmer, G.S. Salvesen, Caspase substrates, Cell Death Differ. 14 (2007) 66–72.
[30] Y. Eguchi, S. Shimizu, Y. Tsujimoto, Intracellular ATP levels determine cell death fate by apoptosis or necrosis, Cancer Res. 57 (1997) 1835–1840.